IJST (2015) 39A3: 325-330
Iranian Journal of Science & Technology

http://ijsts.shirazu.ac.ir

Temperature effects of an asymmetry quantum dot qubit under an applied electric field

Jing-Lin Xiao

Institute of Condensed Matter Physics, Inner Mongolia National University, Tongliao 028043, China
E-mails: xiaojlin@126.com

Abstract

We study the eigenenergies and eigenfunctions of the ground and first excited states (GFES) of an electron strongly coupled to the LO-phonon in an asymmetry quantum dot (AQD) under an applied electric field by using a variational method of the Pekar type (VMPT). This AQD two-level system may be viewed as a single qubit. When the electron is in the superposition state (SS) of the GFES, the effects of the electric field and temperature on the oscillating period (OP), the time evolution of the electron's probability density (PD) and the coherence time (CT) are obtained. Our numerical results show that the electron's PD and its OP will increase (decrease) with increasing temperature in low (high) temperature regime. The electron's PD will decrease (increase) with increasing electron-phonon (EP) coupling strength in low (high) temperature regime. The OP is an increasing function of the electric field and will decrease obviously (increase tardily) with increasing EP coupling strength when the temperature is in lower (higher) rgime. The CT is an increasing function of the electric field, but a decreasing function of the coupling strength.

Keywords: Qubit; temperature; electric field; coherence time; asymmetry quantum dot

1. Introduction

Recently, there has been a great deal of interest in quantum information and quantum computation, and considerable efforts (Harju et al. 2002, Kamada et al. 2004, Liu et al. 2008) have been put on those subjects with a large amount of experimental work (Sikorski et al. 1989, Lorke et al. 1990, Nomura et al. 1992). Meanwhile, many investigators studied their properties in many aspects by a variety of theoretical methods (Li et al. 2006, Li et al. 2010, Li et al. 2013). In quantum computation, two-level quantum dot (QD) system can be viewed as a single qubit, which was studied by many researchers. Quantum interference experiments were performed on a single self-assembled semiconductor QD and a set of quantum operations were combined to realize the single qubit (Bianucci et al. 2004). Using picosecond optical pulses, complete coherent control of a single hole qubit was demonstrated and both free-induction and spin-echo decay were examined (De Greve et al. 2011). A QD qubit architecture, which had a fascinating combination of speed and fabrication, was proposed (Shi et al. 2012). Based on a VMPT, the properties of a QD qubit with a triangular bound potential were investigated. Furthermore, this system has a long decoherence time, which is an attractive property for application in quantum information processing devices (Sun et al. 2009). But this quantum system is very frail due to the interactions between the quantum memories and their surroundings. Therefore, quantum coherence plays a crucial role in the quantum computer. So considerable efforts have been taken to investigate and prolong its time in theory and experiment (Petersson et al. 2010, Bluhm et al. 2011, Hildner et al. 2011). Actually, experiments for any physical system designed for the qubits are performed at a finite temperature, which will cause decoherence in the system (Montina et al. 2008). So, it is necessary and important to consider the temperature effects on the qubits. In our previous work, we have investigated the temperature effects on a QD qubit with parabolic linear bound potential (Chen et al. 2008) and a quantum rod qubit with Coulomb bound potential (Xiao 2013). However, the effects of the temperature and electric field on the AQD qubit have never been investigated, and this the topic of the present manuscript.

2. Theoretical Model

To study the AQD in an electric field, we choose Fig. 1 as the schematic diagram.

Received: 20 June 2014 / Accepted: 8 October 2014

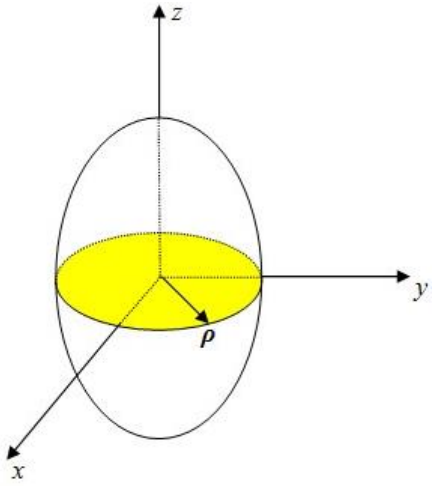

Fig. 1. The schematic diagram of an asymmetry QD

The electron under consideration moves in the dot under a 3D harmonic potential, and is interacts with LO phonons. Under the influence of an electric field $\mathbf{F}$ along the ρ_x direction, the Hamiltonian of the EP interaction system can be written as follows:

$$\begin{aligned} H &= \frac{\mathbf{p}_\rho^2}{2m} + \frac{p_z^2}{2m} + \sum_{\mathbf{q}} \hbar\omega_{LO} a_{\mathbf{q}}^+ a_{\mathbf{q}} \\ &+ \frac{1}{2} m\omega_1^2 \boldsymbol{\rho}^2 + \frac{1}{2} m\omega_2^2 z^2 \\ &+ \sum_{\mathbf{q}} [V_q a_{\mathbf{q}} \exp(i\mathbf{q}\cdot\mathbf{r}) + h\cdot c] - e^* F \rho_x , \end{aligned} \tag{1}$$

where, m is the band mass, ω_1 and ω_2 are the magnitude of the transverse and longitudinal effective confinement strengths of the 3D harmonic potential in the x-y plane and the z direction, respectively. $a_{\mathbf{q}}^+(a_{\mathbf{q}})$ denotes the creation (annihilation) operator of the phonon with wave vector $\mathbf{q}$ and frequency ω_{LO}. $\mathbf{p} = (\mathbf{p}_\rho, p_z)$ and $\mathbf{r} = (\boldsymbol{\rho}, z)$ are the momentum and position vector of the electron, respectively. V_q and α in Eq. (1) are

$$\begin{aligned} V_q &= i\left(\frac{\hbar\omega_{LO}}{q}\right)\left(\frac{\hbar}{2m\omega_{LO}}\right)^{\frac{1}{4}}\left(\frac{4\pi\alpha}{v}\right)^{\frac{1}{2}}, \\ \alpha &= \left(\frac{e^2}{2\hbar\omega_{LO}}\right)\left(\frac{2m\omega_{LO}}{\hbar}\right)^{\frac{1}{2}}\left(\frac{1}{\varepsilon_\infty} - \frac{1}{\varepsilon_0}\right). \end{aligned} \tag{2}$$

We carry out the following Lee-Low-Pines transformation (Lee et al. 1953) to (1)

$$U = \exp\left[\sum_{\mathbf{q}} \left(a_{\mathbf{q}}^+ f_q - a_{\mathbf{q}} f_q^*\right)\right], \tag{3}$$

where $f_q(f_q^*)$ is the variational function, then we obtain

$$H' = U^{-1} H U . \tag{4}$$

Following the VMPT (Pekar 1946, Pekar 1954), the trial wavefunction of the EP system can be separated into two parts, which separately describe the electron and phonon. Then the system's trial GFES' wavefunctions may be chosen (Ding et al. 2012)

$$|\varphi_0\rangle = |0\rangle|0_{ph}\rangle = \pi^{-\frac{3}{4}} \lambda_0^{\frac{3}{2}} \exp\left[-\frac{\lambda_0^2 r^2}{2}\right]|0_{ph}\rangle, \tag{5}$$

$$\begin{aligned} &|\varphi_1\rangle = |1\rangle|0_{ph}\rangle \\ &\left(\frac{\pi^3}{4}\right)^{-\frac{1}{4}} \lambda_1^{\frac{5}{2}} r\cos\theta \exp\left(-\frac{\lambda_1^2 r^2}{2}\right)\exp(\pm i\phi)|0_{ph}\rangle \end{aligned} \tag{6}$$

where λ_0 and λ_1 are the variational parameters. By minimizing the expectation value of the system's Hamiltonian, we then obtain the electron's ground state energy $E_0 = \langle\varphi_0|H'|\varphi_0\rangle$ and the first excited state energy $E_1 = \langle\varphi_1|H'|\varphi_1\rangle$. Then, the two-level system as a single qubit is built up. The SS of the electron can be expressed as

$$|\psi_{01}\rangle = \frac{1}{\sqrt{2}}(|0\rangle + |1\rangle), \tag{7}$$

and the PD of the electron in the AQD is in the following form:

$$\begin{aligned} \mathrm{Q}(r,t) &= |\psi_{01}(r,t)|^2 \\ &= \frac{1}{2}[|\psi_0(r)|^2 + |\psi_1(r)|^2 \\ &+ \psi_0^*(r)\psi_1(r)\exp(-i\omega_{01}t) \\ &+ \psi_0(r)\psi_1^*(r)\exp(i\omega_{01}t)], \end{aligned} \tag{8}$$

where $\omega_{01} = (E_1 - E_0)/\hbar$ is the transition frequency between the GFES. The OP of the PD is

$$T_0 = \frac{h}{E_1 - E_0}. \tag{9}$$

The mean LO phonons number in SS around the

electron is

$$N=\frac{\alpha}{\sqrt{2\pi}}\lambda_0+\frac{3\alpha}{4\sqrt{2\pi}}\lambda_1. \tag{10}$$

Under the dipole approximation, based on the Fermi Golden Rule (Landau et al. 1977), the spontaneous emission rate can be written in the following form:

$$\begin{aligned}\tau^{-1}&=\frac{e^2\Delta E}{3\pi\varepsilon_0\hbar^2m^2C^3}\sqrt{\frac{\varepsilon}{\varepsilon_0}}\left|\langle 0|r|1\rangle\right|^2\\&=\frac{e^2\Delta E}{3\pi\varepsilon_0\hbar^2m^2C^3}\sqrt{\frac{\varepsilon}{\varepsilon_0}}\frac{16\lambda_0^3\lambda_1^5}{\left(\lambda_0^2+\lambda_1^2\right)^5},\end{aligned} \tag{11}$$

where C is the speed of light in vacuum, $\varepsilon(\varepsilon_0)$ is the material (vacuum) dielectric constant, $\Delta E=E_1-E_0$ is the energy separation between the GFES, τ is the CT, and taking $\left(\Re^*\omega_{LO}\right)^{-1}=\left(\frac{e^2r_0^2\omega_{LO}}{3\pi\varepsilon_0\hbar m^2C^3}\sqrt{\frac{\varepsilon}{\varepsilon_0}}\right)^{-1}$ as the unit of CT.

3. Temperature Effect

When the electron is at a finite temperature, the EP system is no longer completely in the ground state. The lattice vibrations excite not only phonon but also electron in the electric field and harmonic potential. The statistical average value of different states can be used to describe the properties of polaron. According to the quantum statistics theory, the statistical average number of the optical phonons is

$$\overline{N}=\left[\exp\left(\frac{1}{K_BT}\right)-1\right]^{-1}, \tag{12}$$

where K_B is the Boltzmann constant and T denotes the temperature of the system. With the consideration mentioned above, the values of λ_0 and λ_1 determined by Eq. (10) relates not only to the value of N but also to the value of $\overline{N}$, which should be self-consistently calculated with Eq. (12). In such a way, we can obtain the relation between λ_0 and λ_1 and the temperature T. From Eqs. (8), (9) and (11) we can see that the PD, the OP and the CT of the electron in an AQD all depend on the variational parameters λ_0 and λ_1, and then are related to the temperature T.

4. Results and Discussion

As usual, we choose the usual polaron unit $(\hbar=2m=\omega_{LO}=1)$, and the numerical results of the electron's PD $Q(r,t)$ and its OP T_0 versus the temperature T, the electric field F, the EP coupling strength α are presented in Figs. 2-5. Also, the numerical results of the CT τ versus the electric field F and the EP coupling strength α are presented in Fig. 6. In Figs. 2-6, taking $\hbar\omega_{LO}$, ω_{LO}, $\hbar\omega_{LO}/e^*r_0$, $(\omega_{LO})^{-1}$, r_0 and $(\Re^*\omega_{LO})^{-1}$ as the units of energy, vibrational frequency, electric field, OP, the effective confinement length and the CT, respectively. The effective confinement length's magnitude is in the nanoscale.

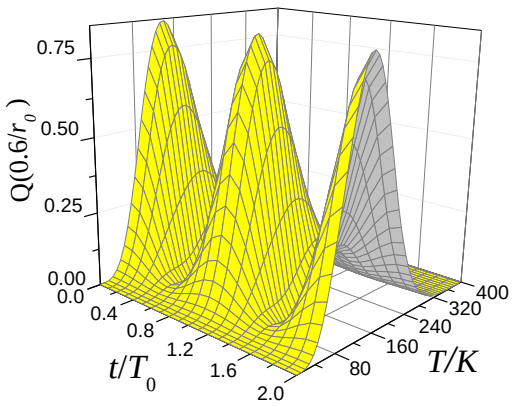

Fig. 2. The time evolution of the electron's probability density versus the temperature. (units of temperature: K, units of time: T_0)

Figure 2 shows the electron's PD versus the temperature and the time when the electron is located in $r=0.6$ for $\alpha=6.5$, $F=1.0$, $l_1=0.2$, $l_2=0.3$ and $\cos\theta=0.75$. We find that the electron oscillates with an OP $T_0=h/(E_1-E_0)$ in the AQD. At the same time, we can easily see that the electron's PD will increase (decrease) with increasing temperature at low (high) temperature region. This can be explained as follows. The thermal motion's velocity of the electron will increase with increasing temperature, which will cause its probability in the SS to increase. Then, the electron will interact with more phonons, which will lead to the destruction of the SS. In the low temperature regime, the contribution from the former is greater than that of the latter, so the electron's PD will increase with

increasing temperature. Opposite tendency emerges, however, when the system is in the high temperature regime, which will make the electron's PD decrease with increasing temperature. Here it can be seen that we can aggrandize the electron's PD by tuning the temperature of the AQD system. In low (high) temperature regime, we allow the AQD system work in the higher (lower) temperature to amplify the PD.

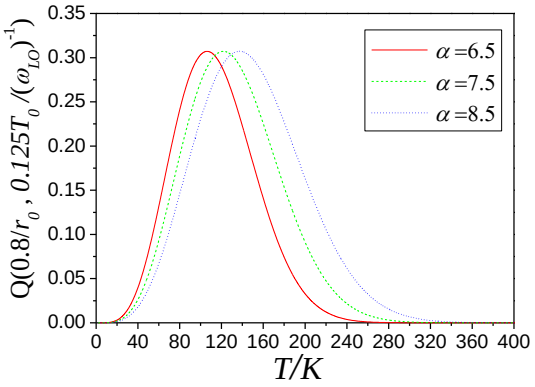

Fig. 3. The probability density versus the temperature for different values of the EP coupling strength (units of temperature: K). The solid, dashed and dotted lines correspond to cases of the EP coupling strength $\alpha = 6.5$, $\alpha = 7.5$ and $\alpha = 8.5$, respectively

Figure 3 represents the electron's PD as a function of the temperature and the EP coupling strength when the evolutionary time t is $0.125\ T_0$ and the electron is situated in $r = 0.8$ for $F = 3.0$, $l_1 = 0.8$, $l_2 = 0.6$ and $\cos\theta = 0.75$. The solid, dashed and dotted lines correspond to the cases of the EP coupling strength $\alpha = 6.5$, $\alpha = 7.5$ and $\alpha = 8.5$, respectively. It illustrates that the electron's PD will decrease with increasing EP coupling strength in low temperature zone. This is because the influence of the EP coupling strength on the first excited state is weaker than that on the ground state in low temperature regime, the energy gap between these two energy states will increase with increasing EP coupling strength. That is to say, the electron's transition probability between relevant states will decrease with increasing EP coupling strength in low temperature zone, which will lead to the decrease of the electron's PD. Moreover, we interestingly find that the electron's PD will increase with increasing EP coupling strength at high temperature region due to the novel quantum size confining effect of the AQD system. Here we can see that by changing the EP coupling strength of the material we can adjust the PD of the two-level quantum system. So, we may choose materials with smaller (larger) EP coupling strength in the low (high) temperature regime to maximize the PD.

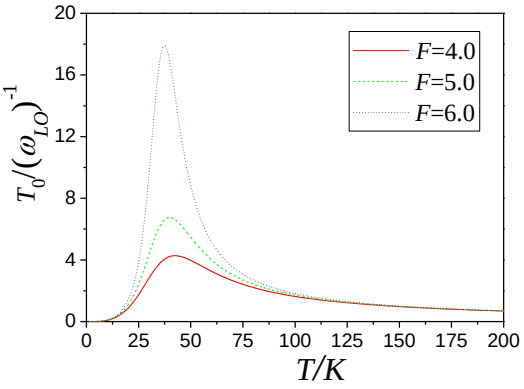

Fig. 4. The oscillatory period versus the temperature for different values of the electric field (taking K, $(\omega_{LO})^{-1}$ and $\hbar\omega_{LO}/e^{*}r_0$ as the units of the temperature, oscillating period and electric field). The solid, dashed and dotted lines correspond to cases of the electric field $F = 4.0$, $F = 5.0$ and $F = 6.0$, respectively

Figure 4 indicates the OP versus the electric field and the temperature for $\alpha = 7.0$, $l_1 = 1.0$, and $l_2 = 1.5$. The solid, dashed and dotted lines correspond to the cases of the electric field $F = 4.0$, $F = 5.0$ and $F = 6.0$, respectively. From Fig. 4. we can easily find that (i) at low (high) temperature regime the OP will increase (decrease) with increasing temperature; and (ii) the OP is an increasing function of the electric field and it becomes insensitive with the electric field in high temperature zone. Our theoretical results are in good agreement with the results of Li et al. 2001 and Li et al. 2001, which were obtained for an InAs/GaAs QD in the framework of the effective-mass envelope function theory. Furthermore, because the influence of the temperature, we predict a few new phenomena. Here it can be seen that we may enlarge the OP by increasing the external applied electric field and controlling the temperature of the two-level system at a proper parameter value.

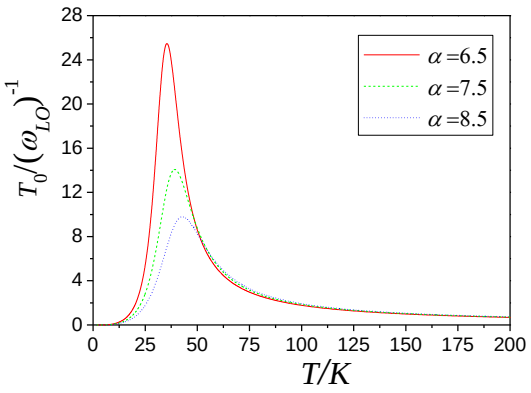

Fig. 5. The oscillating period versus the temperature for different values of the EP coupling strength (taking K and $(\omega_{LO})^{-1}$ as the units of the temperature and the oscillating period). The solid, dashed and dotted lines correspond to cases of the EP coupling strength $\alpha = 6.5$, $\alpha = 6.5$ and $\alpha = 8.5$, respectively

The OP as a function of the temperature and the EP coupling strength is depicted in Fig. 5. for $F = 6.0$, $l_1 = 1.0$, and $l_2 = 1.5$. The solid, dashed and dotted lines correspond to the cases of the EP coupling strength $\alpha = 6.5, \alpha = 7.5$ and $\alpha = 8.5$, respectively. It shows that the OP will rise (drop) with increasing temperature in low (high) temperature region as depicted in Fig. 4. We can also see that the OP will decrease visibly in the low temperature regime with increasing EP coupling strength. The reason is that the increase in the first excited state by increasing the EP coupling strength is smaller than that in the ground state. Thus, the energy spacing between them will increase with increasing EP coupling strength, which will cause the reduction of the OP. Moreover, we find that the OP will increase slowly with increasing EP coupling strength in the high temperature region. These phenomena are all attributed to the interesting quantum size confining effect of the AQD system. Here we can find that by changing the temperature and EP coupling strength of the material the OP of the two-level quantum system can be adjusted.

Figure 6 plots the CT as a function of the electric field and the EP coupling strength for $l_1 = 1.0$ and $l_2 = 1.5$. It turns out that the CT increases with the increase of the electric field. This is because the electric field is stronger in the first excited state than that in the ground state and the energy spacing between the GFES decreases with increasing electric field. So the CT increases. This result is in agreement with the results of Li et al. 2001, which were obtained by using the effective-mass envelope function theory, Fig. 6 also indicates that the CT is a decreasing function of the EP coupling strength. The reason is that, the energy spacing increase with increasing coupling strength and the CT decrease.

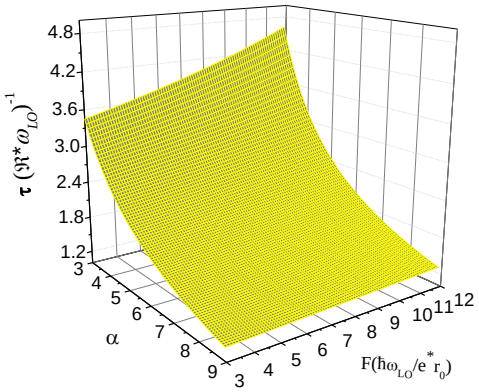

Fig. 6. The coherence time versus the electric field and the EP coupling strength (taking $(\Re^*\omega_{LO})^{-1}$ as the units of the coherence time)

As compared to other similar theoretical methods mentioned above, the VMPT is quite simple and convenient with very clear physical pictures. Under this technique, the adopted trial function is the Gaussian one, which is very close to the real wavefunction in QD and then the obtained results are very accurate. It has been demonstrated to be a good method to investigate problems of the strong electron-coupling.

5. Conclusions

We have studied the temperature effect and the time evolution of the PD and its OP of an electron strongly coupled to the LO phonons under an applied electric field in an AQD with a 3D harmonic potential. The eigenenergies and eigenfunctions of the GFES of an electron have been calculated in the presence of an electric field. The numerical results indicate that the electron's PD and its OP will increase (decrease) with increasing the temperature at low (high) temperature region. The CT is an increasing function of the electric field, but it is a decreasing one of the coupling strength. The electron's PD oscillates in the AQD with a certain period, and to maximize it we may choose materials with the smaller (larger) EP coupling strength in the low (high) temperature regime. The OP is effectively prolonged by increasing the external electric field and choosing the smaller EP coupling strength in the whole temperature regime.

Acknowledgments

This project was supported by the National Science Foundation of China under Grant No. 11464034 & 11464033.

References

Bianucci, P., Muller, A., Shih, C. K., Wang, Q. Q., Xue, Q. K., & Piermarocchi, C. (2004). Experimental realization of the one qubit Deutsch-Jozsa algorithm in a quantum dot. *Physical Review B*, 69(16), 161303.

Bluhm, H., Foletti, S., Neder, I., Rudner, M., Mahalu, D., Umansky, V., & Yacoby, A. (2011). Dephasing time of GaAs electron-spin qubits coupled to a nuclear bath exceeding 200[thinsp][mu]s. *Nature Physics*, 7(2), 109–113.

Chen, Y. J., & Xiao, J. L. (2008). The temperature effect of the parabolic linear bound potential quantum dot qubit. *Acta Phys. Sin.*, 57(11), 6758–6762.

De Greve, K., McMahon, P. L., Press, D., Ladd, T. D., Bisping, D., Schneider, C., Kamp, M., Worschech, L., Hofling, S., Forchel, A., & Yamamoto, Y. (2011). Ultrafast coherent control and suppressed nuclear feedback of a single quantum dot hole qubit. *Nature Physics*, 7(11), 872–878.

Ding, Z. H., Sun, Y., & Xiao, J. L. (2012). Optical phonon effect in an asymmetric quantum dot qubit. *International Journal of Quantum Information*, 10(07), 1250077.

Harju, A., Siljamäki, S., & Nieminen, R. M. (2002). Two-electron quantum dot molecule: composite particles and the spin phase diagram. *Physical Review Letters*, 88(22), 226804.

Hildner, R., Brinks, D., & van Hulst, N. F. (2011). Femtosecond coherence and quantum control of single molecules at room temperature. *Nature Physics*, 7(2), 172–177.

Kamada, H., & Gotoh, H. (2004). Quantum computation with quantum dot excitons. *Semiconductor Science and Technology*, 19(4), S392.

Landau, L. D. & Lifshitz, E. M. (1977). *Quantum mechanics (non-relativistic theory)*. New York: Pergamon Press.

Lee, T. D., Low, F. E., & Pines, D. (1953). The motion of slow electrons in a polar crystal. *Physical Review*, 90(2), 297–302.

Li, H. j., Yin, J. W., & Xiao, J. L. (2013). The triangular and coulomb bound potential quantum dot qubit. *Journal of Low Temperature Physics*, 172(3-4), 266–273.

Li, S. S., & Xia, J. B. (2006). Electronic structure and binding energy of a hydrogenic impurity in a hierarchically self-assembled GaAs⁄AlxGa1−xAs quantum dot. *Journal of Applied Physics*, 100(8), 083714.

Li, S. S., Long, G. L., Bai, F. S., Feng, S. L., & Zheng, H.-Z. (2001). Quantum computing. *Proceedings of the National Academy of Sciences of the United States of America*, 98(21), 11847–11848.

Li, S. S., Xia, J. B., Liu, J. L., Yang, F. H., Niu, Z. C., Feng, S. L., & Zheng, H. Z. (2001). InAs/GaAs single-electron quantum dot qubit. *Journal of Applied Physics*, 90(12), 6151–6155.

Li, W. P., Yin, J. W., Yu, Y. F., Wang, Z. W., & Xiao, J. L. (2010). The effect of magnetic on the properties of a parabolic quantum dot qubit. *Journal of Low Temperature Physics*, 160(3-4), 112–118.

Liu, Y. F., & Xiao, J. L. (2008). The effects of LO phonons on charge qubit. *Physica B-Condensed Matter*, 403(18), 3013–3017.

Lorke, A., Kotthaus, J. P., & Ploog, K. (1990). Coupling of quantum dots on GaAs. *Physical Review Letters*, 64(21), 2559–2562.

Montina, A., & Arecchi, F. T. (2008). Quantum decoherence reduction by increasing the thermal bath temperature. *Physical Review Letters*, 100(12), 120401.

Nomura, S., & Kobayashi, T. (1992). Exciton-LO-phonon couplings in spherical semiconductor microcrystallites. *Physical Review B*, 45(3), 1305–1316.

Pekar, S. I. (1946). Local quantum states of electrons in an ideal ion crystal. *Zhurnal Eksperimentalnoi I Teoreticheskoi Fiziki*, 16(4), 341–348.

Pekar, S. I. (1954). *Untersuchungen uber die elektronentheorie der kristalle*. Berlin: Akademie Verlag.

Petersson, K. D., Petta, J. R., Lu, H., & Gossard, A. C. (2010). Quantum coherence in a one-electron semiconductor charge qubit. *Physical Review Letters*, 105(24), 246804.

Shi, Z., Simmons, C. B., Prance, J. R., Gamble, J. K., Koh, T. S., Shim, Y.-P., Hu, X., Savage, D. E., Lagally, M. G., Eriksson, M. A., Friesen, M., & Coppersmith, S. N. (2012). Fast hybrid silicon double-quantum-dot qubit. *Physical Review Letters*, 108(14), 140503.

Sikorski, C., & Merkt, U. (1989). Spectroscopy of electronic states in InSb quantum dots. *Physical Review Letters*, 62(18), 2164–2167.

Sun, J. K., Li, H. J., & Xiao, J. l. (2009). Triangular bound potential quantum dot qubit. *Physica B: Condensed Matter*, 404(14–15), 1961–1964.

Xiao, J. L. (2013). Influences of temperature and coulomb bound potential on the properties of quantum rod qubit. *Superlattices and Microstructures*, 60248–256.